Thermo-mechanical effects induced by lightning on carbon fiber composite materials

B. Lepetit*, C. Escure, S. Guinard,
I. Revel, G. Peres
EADS, Innovation Works
Bâtiment Campus engineering
BP90112, 31703 Blagnac Cedex, France
* bruno.lepetit.external@eads.net

Y. Duval
EADS, Innovation Works
12 rue Pasteur
BP76, 92152 Suresnes Cedex, France

Abstract

The present paper describes new experimental and modelling results aiming at an improved understanding of the damage mechanisms induced by lightning strikes in carbon fiber composite materials. We focus on the effects of the impulse components which are less understood and on a possible mechanical origin to these phenomena. A new kind of instrumentation was implemented in direct effect tests. A high speed digital camera providing 500 000 frames per second with 312 x 260 pixel resolution was used to observe the initiation and development of lightning D waveforms on the tested materials. Interferometric time resolved measurements of the speeds and deflections of the panels submitted to the strikes were performed, from which information on the pressure developing at the surface of the tested samples during strikes was extracted. These test results were interpreted in the light of thermo-mechanical simulations, giving stresses and strains in the material for different kinds of energy deposits. These results provide new insight on the physical origin – thermal versus mechanical - of the damage. We study in particular the beneficial effect of metal deposits and detrimental effect of paint layer on the damage. We show that paint has an inertial confinement effect, which enhances pressure on the surface. A simple model for this enhancement is proposed, derived from similar ones used to describe shock generation by laser impulses in confined materials. This enhancement may be responsible for increased damages in presence of paint.

1. Introduction.

The extended use of carbon fiber composite (CFC) materials in new generation aircraft requires to control the behaviour of such materials subjected to direct lightning strikes. This is usually done with tests : samples are subjected to discharges representative of lightning and from the analysis of the induced damage it is decided whether the material is adequately protected against lightning threat or not. It has been observed that the level of damage on unprotected CFC is usually high, and adequate protections have to be designed. Typically, it consists in adding some sort of metallization on the material. An understanding of the damage mechanisms would be useful to guide the material design, and the present paper is a contribution to improved understanding of the physical mechanisms inducing lightning damage on CFC materials.

A lightning strike amounts in a fast energy deposit in the material. Its effect is usually described with thermal concepts: the energy deposit induces fast temperature increase, which in turn can induce phase transitions. Damage can then be described as the appearance of liquid or vapour phases in the material. This approach is well adapted for metallic materials but is more questionable in the case of composites [1-2]. Indeed, in such cases, although burnings and surface damage may be explained by such thermal processes, delamination and in depth damage may be induced by more complex processes involving mechanical effects in addition to thermal ones. The thermal model therefore needs to be supplemented by mechanical

concepts to provide a valuable understanding of damage processes.

A first step along this line was made in ref. [3], focusing exclusively on mechanical effects. Panels subjected to lightning direct attachment tests were instrumented by mechanical and optical means such that the mechanical impulse (i. e. the force imparted by the electrical arc on the material integrated over time) has been extracted from deflection measurements by comparison with purely mechanical tests. Impulses typically of the order of 1 N.s or less were obtained. No clear correlation between these measurements and damage was achieved.

Ref. [4] elaborated further along the line of ref. [3] and provided time resolved deflections at different points in the material, using high resolution visar interferometric optical technologies. A model was developed to extract from measured deflection the mechanical impulse induced by the strike. Moreover, a thermo-mechanical model was developed to describe damage in the material.

The present paper proposes further progress along this line. New instrumented lightning tests were performed on CFC panels with different types of surface protections and paints. A high speed camera was used to observe the development of damage on the front side of the panel in real time. Visars were positioned on the rear side of the panels to record deflection and speed of the panels at different points near the arc attachment location, as a function of time. A mechanical model was then used to extract information on the load distribution on the surface of the material applied by the lightning strike. These results are described in section 2. Section 3 proposes a simple model which provides orders of magnitude of applied stresses on the surface of the material by the lightning strike, and describes preliminary results of a full thermo-mechanical model. It points out a plausible explanation for the detrimental effect induced by the presence of paint on the material.

2. Instrumented tests

2.1 Instrumentation

The tested CFC samples were T700/M21, 8 uni-directional plies with a quasi-iso lay-up, size 450 x 450 x 2 mm^3. Metallic protection consisted in expanded copper foils (ECF), 73 or 195 g/m^2. These samples were covered or not by a standard paint system 200 µm thick. They were subjected to standard arc attachment tests, with a lightning waveform of D type reaching a maximum in the range 94-98 kA, within nearly 20 µs, and with a total duration of less than 100 µs. The action integral is in the range 0.28-0.30 10^6 A^2s.

A Shimadzu HPV1 camera located inside a faradized box equipped with a zoom (focal 300 mm) was used to observe arc development and real-time damage processes on the front side. Different optical filters were used to avoid saturation of the sensors by the light emitted by the electrical arc. For each strike, 100 images were recorded with a 2 µs periodicity, and with a 0.5 µs pause duration.

Speed and deflection of the plate were measured with a 5 heads visar system. 4 heads form a square having a side of 50 mm and the 5^{th} head is at the center of the square. The square center is located close to the expected strike location at the center of the sample, but on the opposite side of the material. Each head emits a 1550 nm IR laser beam, which reflects on the sample and interferes with a reference beam. Speed and displacement of the samples at the 5 points are obtained by analysis of the displacement of the interference fringes. Notice that such an interferometric system is extremely accurate. It measures speeds ranging from 10^{-2} to $3\ 10^3$ m/s with an error less than 1 %. Signal is recorded on a 2 milliseconds duration with a temporal resolution of 1 nanosecond.

2.2 Results

2.2.1 Pictures

We present pictures corresponding to painted composite and ECF 73. Fig. 1 shows the first 4 images after initition, separated by 2 µs. We see a fast expanding luminous arc first cylindrical and then with a characteristic pear shape. Right part of each frame shows an attenuated image of the arc, by reflection on the sample. This reflected image shows a cylindrical hot core for the arc, which may be the region where current flows predominantly. The pear shape may be characteristic of a plasma jet developing from the electrode to the sample.

Fig. 2 presents pictures taken in the extinction phase, nearly 78-88-98-108 µs after initiation. The arc is almost extinguished and does not produce any more a significant amount of light. An explosion of the paint surface layer is clearly seen. It is thus interesting to notice that damages, at least surface ones, start to appear early, less than 100 µs after initiation of the arc.

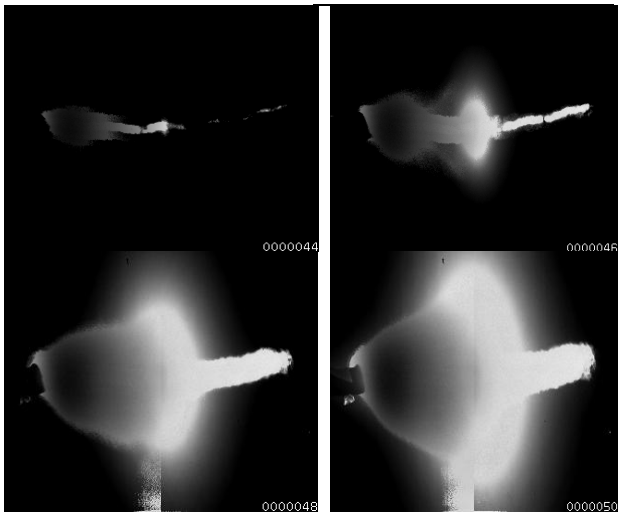

Figure 1: Pictures of the strike in its initiation phase. Ordered from top left to bottom right, the pictures are separated by 2 µs. The arc was initiated less than 2 µs before the first picture. Right part of the picture corresponds to the reflected image of the arc on the sample. The electrode is on the left.

The explosion is probably induced by a pressure build-up under the paint layer. This is an experimental evidence of the surface explosion which was up to now only an hypothetical contributor to lightning mechanical effects [3].

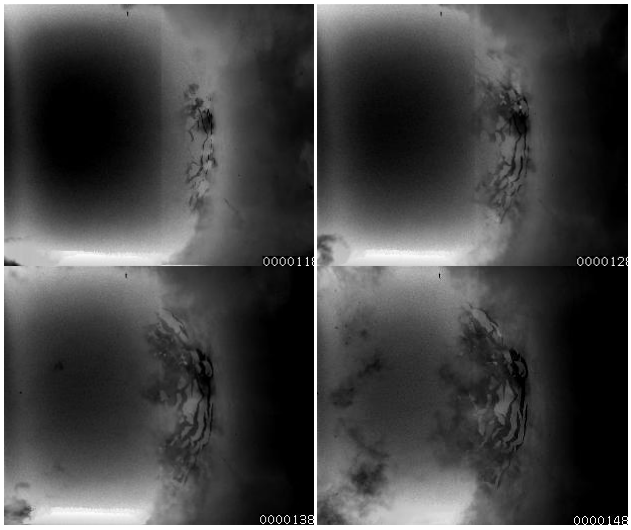

Figure 2: Pictures of the strike in its extinction phase. Ordered from top left to bottom right, the pictures are separated by 10 µs. The first one corresponds to nearly 78 µs after initiation.

Moreover, the presence of paint may confine the plasma induced by sudden Joule heating of the material beneath the paint. This may enhance stress and subsequent damages in the material. We propose in section III a model to describe this process, where the confinement has an inertial origin.

2.2.2 Visar measurements

Visars provide deflection and speed of the samples. We show on fig. 3 the speed of the sample measured by the visar closest to the strike point.

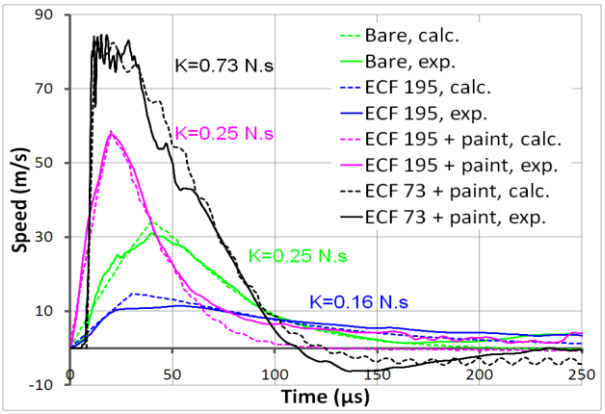

Figure 3: Speed of the sample at the strike point as a function of time. Different samples are considered. Continuous line : experimental result. Dashed line : model. K is the impulse (in N.s) corresponding to the surface pressure integrated over area and time.

Four different samples are considered on fig. 3, the same carbon fiber material with different surface states as described before. In all cases, speed first increases, within a time ranging between 4 to 40 µs, before decreasing. The rate of increase at short times is directly related to a pressure applied on the surface material due to lightning. The rigidity of the plate comes later into play to slow down the motion.

We performed calculations to relate the measured speeds and deflections to the pressure applied on the surface. As will be discussed below, there are several possible contributors to this surface pressure, and little is known on the spatial and temporal distribution of each them. We therefore decided to represent the applied pressure in the simplest possible way as being constant over its application time T and with a gaussian spatial distribution of radius r centered around the strike point, where the pressure has an amplitude A. We performed iteratively computations of the deflection of the plate using the mechanical software ABAQUS, changing the values of the 3 pressure parameters T, r, A until a

good agreement between computed and measured speeds was obtained. The result achieved can be appreciated on fig. 3 by comparing continuous (measured) and dashed (computed) results. From these data, the impulse (in N.s) imparted to the material can be defined as: $K=\pi r^2 A T$. Similar orders of magnitude for this impulse had been found previously [3].

		r (cm)	A (bar)	T (µs)	K(N.s)
1	Bare : no prot., no paint	2.2	40	40	0.25
2	ECF 195 g/m², no paint	3.2	17	30	0.16
3	ECF 195 g/m², 200 µm paint	1.6	160	20	0.25
4	ECF 73 g/m², 200 µm paint	2.9	700	4	0.73

Table 1 : The spatial, temporal and amplitude of the applied surface pressure which provide speeds in good agreement with measured results, see fig. 3.

It is interesting to notice that the results of table 1 are consistent with the common understanding of protection and paint effect. Adding an ECF on a bare material do reduce the applied pressure and impulse (compare sample 1 with 2). Painting the protected sample restores the impulse to its initial value but with a more intense pressure applied on a shorter time (sample 3 vs 1). Finally, the lighter protection results a much stronger pressure and impulse applied during a shorter time (sample 4 versus 3).

Different contributions to this applied pressure had already been described [3]: Laplace magnetic forces, overpressure in the arc column... Our present results indicate a strong dependence of the speed, and consequently of applied pressure, on the surface state. In particular, the 2 samples covered with paint undergo a higher acceleration, meaning a larger applied pressure, than the unpainted ones. This provides a quantitative assessment of the well documented detrimental effect of paint on composite materials. This detrimental effect may be due to an enhancement of the magnetic and arc overpressure due to a reduced arc radius, the paint acting as a dielectric layer confining the arc root. Another possible explanation is to assume that the presence of paint induces a new contribution to lighning overpressure which adds to the others, namely a surface explosion of the protection layer through which most of the applied current flows. This induces violent Joule effect, fast development of a plasma underneath the paint, which acts as an inertial confinement material. The fact that we observe surface explosion on pictures when paint is present (see fig. 2) is an empirical evidence of this confined surface explosion. In the next section, we develop a simple model providing more support to this idea of confined surface explosion as a contribution to surface pressure and damage enhancement.

3. Models

3.1 Surface explosion model

The creation of a high pressure surface explosion induced by a sudden local energy deposit is a well documented phenomenon. For instance, it is well known that energy brought by a powerful pulse laser on the surface of a material can generate a shock wave, propagating through the material and inducing damage, and that this process will get worse if it takes place in a confined medium. There are models available to describe such phenomena in the literature [5], and the purpose of the present section is to study how such models can be adapted to the present context. For simplicity, we consider a one dimensional model depending only on the height perpendicular to the material surface.

We therefore consider a protection layer (copper foil) of thickness $L(t)$ (t :time), bounded on one side by the composite material of mass per unit area m_M and on the other side by paint of mass per unit area m_C. As energy is injected in the protection layer through Joule effect, pressure $P(t)$ increases in the protection, and this pressure increase widens the gap $L(t)$ between material and paint. Indeed, Material and paint layers are pushed away from each other and Newton's equation reads:

$$\frac{d^2L}{dt^2} = \frac{1}{\mu}P \qquad \text{(eq. 1)}$$

where μ is the reduced mass : $\mu = m_C\ m_M/(m_C+m_M)$. Eq. 1 is a momentum conservation equation describing an inertial confinement of the pressure by the surrounding media. This equation must be supplemented by an energy conservation equation:

$$w = P\frac{dL}{dt} + \frac{d}{dt}(LE_i) \qquad \text{(eq. 2)}$$

which expresses the fact that the power per unit area w brought in by Joule effect can be used

either in mechanical work PdL/dt, or in heating up the protection layer and increase its internal energy E_i. We need a state equation to relate the internal energy to pressure, so that the system of 2 equations (eq. 1 + eq. 2) only has 2 unknowns (*P(t)* and *L(t)).* If we assume that a fraction α of the internal energy corresponds to the kinetic energy of the atomic and molecular species and contributes to pressure, the rest corresponding to internal energy (ionization…), the simple state equation is:

$$\alpha E_i = \frac{3}{2} P \qquad \text{(eq. 3)}$$

A reasonable value for *α* was obtained from the thermodynamical data of P. Kovitya [6]. Assuming local thermal equilibrium, the composition of the plasma in terms of neutral and ionic species is computed as a function of temperature and pressure. Physical properties like densities and enthalpy can then be computed [6], and we extract from them the ratio E_i/P. This ratio turns out to be fairly constant in a wide range of temperature and pressure and equal to 6. This provides : α=0.25.

$L(t)$ and $P(t)$ can now be obtained from the solution of the coupled differential equations (eq. 1 + eq. 2) using a standard 4th order Runge-Kutta integrator, once the input Joule power is given. We assume a simple axi-symmetric model depending of the arc radius R. For a radius *r*<*R*, the radial current density is given by: $j = I\frac{r}{2L\pi R^2}$ and for *r*>*R*: $j = I\frac{1}{2L\pi r}$. I is the time dependant injected current (D-type waveform). Integrating the Joule power dissipated by this current distribution over a cylindrical protection layer limited by *rmx* (defining an effective area on which pressure is applied) and dividing by the area $\pi\ rmx^2$ in which the power is injected, we obtain :

$$w = \frac{1 + 4\ln(\frac{rmx}{R})}{8\pi^2 rmx^2} Z_s I^2 \qquad \text{(eq. 4)}$$

where Z_s is the electrical surface impedance.

When the material is not covered with paint, there is no inertial confinement. Instead, there is a shock wave generated at the surface of the material which propagates through the material on one side, and through the air on the other side. The shock wave generates in its wake an overpressure given by Rankine-Hugoniot equation which must be used instead of Newton's equation (eq. 1):

$$\frac{dL}{dt} = \frac{1}{Z} P \qquad \text{(eq. 5)}$$

Z is the equivalent mechanical impedance : $Z=Z_C\ Z_M/(Z_C+Z_M)$.The impedances in air and material are the product of density and shock propagation speed, given by a constant in the material and by :

$$D_C = \left(\frac{\gamma+1}{2}\frac{P}{\rho_C}\right)^{\frac{1}{2}} \qquad \text{(eq. 6)}$$

in air, assuming a perfect gas of density ρ_C adiabatic index $\gamma\approx$1.4.

The results of this surface explosion model, for both the confined and unconfined cases, are given on fig. 4. The same four samples as in section 2 are considered and they allow to study the effects of paint and protection. We consider electrical surface impedances given by: Zs=31, 5 and 1.5 mΩ for the bare, ECF 73 and ECF 195 samples, respectively. We set *rmx* to the value r given in table 1. It corresponds to the radius on which pressure applies. We use an arc radius (defining the disk in which current is injected) *R=6 mm*, corresponding approximately to the radius of high luminosity, as seen by reflection on the right part of each picture of fig. 1.

The comparison of fig. 4 with the experimental results of fig. 3 shows that the present model, although very simple, grasps the essential features of the physical processes at play. The confining effect of paint induces a faster increase of pressure, which induces the faster increase of speed observed experimentally. Maximum pressure is reached earlier when paint is present (near 5 *μs* in the model), and this appears as an earlier time to reach maximum speed on fig. 3. In the confined case, the pressure temporal profile is much faster than the energy input profile, proportional to the injected current squared, which peaks at 20 μs. By contrast, pressure profile is slightly slower than the energy input in the unconfined case. These considerations are consistent with the pressure application times given in table 1, shorter in the confined cases.

The impulse *K* (in N.s) can be obtained from the models by simple time integration. We obtain 0.36, 0.07, 0.13 and 0.54 N.s for the cases bare, ECF 195, ECF 195 + paint, ECF 73 + paint, respectively. The agreement with table 1 is again

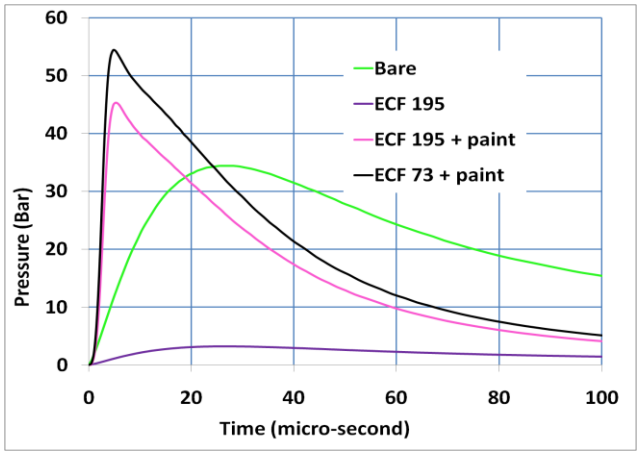

Figure 4: Pressure at the surface of the composite material, as a function of time, obtained with the simple surface explosion model.

satisfactory. Results are of the same order of magnitude. Except for case "Bare", the surface explosion model provides a smaller value than table 1. This is consistent with the fact that the impulse of table 1, extracted from visar measurements, includes all contributions, magnetic, arc overpressure, and surface and internal explosions. This shows however that the surface explosion is important and cannot be neglected with respect to the others.

Pressure amplitudes *A* given in table 1 can also be compared with those of fig. 4. Our model reproduces again the trends, larger amplitude in the confined case. In fact, we could check by performing systematic simulations that within the frame of this model, the maximum pressure, for a given confined/unconfined configuration, is proportional to the square root of the injected energy per unit surface *w* (eq. 4). The painted cases, ECF 195 and ECF 73, give fairly similar amplitude because, although the electrical surface impedance is more than three times larger in the ECF 73 case, the radius defining the area where energy is injected is also larger (table 1), so that the injected energy per unit area are similar. In the unpainted case, the pressure is much smaller in the ECF 195 case than in the bare case, because surface impedance is smaller and and radius larger, both factors contributing to the reduction of injected power per unit area. Notice however that the surface explosion model does not provide a quantitative agreement with the amplitudes given in table 1. This may be due in part to the too crude representation of the applied pressure used to fit the visar signals, but there is no doubt that a simple one dimensional model cannot describe the whole complexity of the physical phenomena. We consider in the next section preliminary results of a more complete thermo-mechanical model.

3.2 Thermo-mechanical model

We used ABAQUS-explicit multi-physics Finite Element software to perform a two-dimensional axi-symmetric model of the problem. We consider the ECF195 + paint configuration. The mesh consists of 11000 rectangular elements (22 through the thickness). We consider a cylindrical portion of the material with radius 50 mm only. The results of the model should be expected to be accurate at short times only, before the strain initially induced at the center reaches the border of the meshed portion. The mechanical properties of the composite stack are described in terms of the 9 well known material characteristics of an elastic orthotropic medium, homogeneized from Young, Poisson and shear moduli of each of the 8 plies. The injected power considered is the Joule effect in the protection layer resulting from the simple axisymmetric current distribution described in the previous section. It is thus maximum at a distance from the symmetry axis corresponding to the arc radius. The same simple state equation as in the previous section is used to relate pressure to the internal energy.

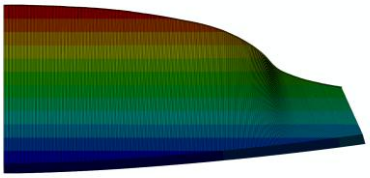

Figure 5: Deformation of the axisymmetric structure at t=100 µs, obtained with ABAQUS. The left border corresponds to the axis of symmetry, the radius of the portion of the sample shown is 50 mm. Bottom part corresponds to the material, the top part to the paint layer flying away from the material. The metal protection domain underneath the paint layer is expanding due to Joule heating. Simultaneously, the material is bending under the applied surface pressure. Each colored band represents a displacement range of 2.5 mm.

The deformation of the structure at 100 µs is shown on fig. 5. This time corresponds nearly to the ones of fig. 2, which shows pictures of the exploding paint. This is qualitatively in agreement with fig. 5, which shows the paint layer receding away from the material. Indeed, due to Joule effect, the protection layer underneath is

expanding while remaining inertially confined by the paint layer. Obviously, our model does not describe the breaking up of the paint layer into pieces, but describes adequately their global motion.

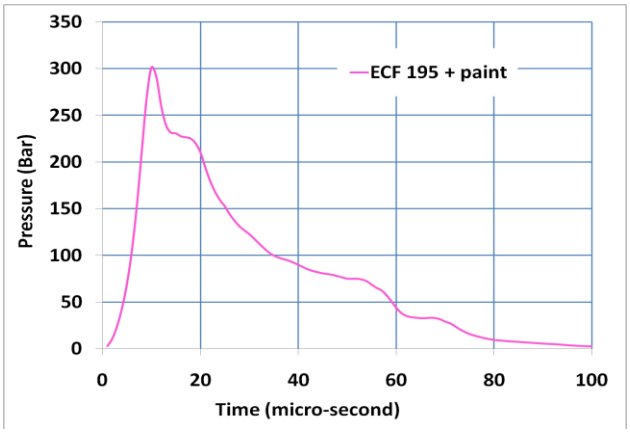

Figure 6: Pressure on the surface as a function of time for r=6 mm (arc root radius), obtained with ABAQUS.

ABAQUS also provides the pressure at each point of the surface of the material. An example is given in fig. 6 which shows pressure as a function of time for r=6 mm, the arc root radius. This corresponds to the point where pressure is highest. One can compare this result with table 1 or fig. 4 (ECF 195 + paint). Trends are in good agreement: pressure reaches its maximum faster than the input energy in both cases, in nearly 10 µs in the present thermomechanical model. Keeping in mind that the simple model of the previous section provides some average value over an area of radius *rmx*, the present max value for pressure, 300 bar at 10 µs at the location of highest pressure, is consistent with the spatially averaged value of 45 bar found on fig. 4.

4. Perspectives

We described in this paper the results of a combined experimental and theoretical study of the thermo-mechanical effects of a lightning strike on a material. Ultra fast cameras allowed us to gain qualitative information on the initiation of the arc and on the explosion occurring later on the surface. Visars provided information on the deflection of the material and its speed, from which we obtained information on the extension, duration and intensity of the surface explosion. These data were confronted to a simple one dimensional explosion model and a more involved thermo-mechanical description, which provided a consistent picture of the phenomena. We focused in particular on the confining role of paint.

This work is only a first step toward a more complete description of the complex lightning direct effects. An enriched thermo-mechanical model should include the other contributions to pressure and energy inputs. Stresses and strains resulting in the material from such input should then be computed with an ABAQUS type software, and the stresses in the material should be compared to damage thresholds. Such a work should provide a global understanding of the damage processes and suggest means to limit them in efficient ways.

5. References

1. “A computational approach to predicting the extent of arc root damage in CFC panels”, Jennings N. and Hardwick C. J. , *15th Int. Aerospace and Ground Conf. on Lightning and Static Electricity (Atlantic City, 1992)* pp 41.1–41.8

2. “A numerical modelling of an electric arc and its interaction with the anode: part III. Application to the interaction of a lightning strike and an aircraft in flight”, F. Lago, J. J. Gonzalez, P. Freton, F. Uhlig, N. Lucius and G. P. Piau, J. Phys. D: Appl. Phys. **39** (2006) 2294–2310

3. ”Impulse Effects during Simulated Lightning Attachments to Lightweight Composite Panels”, S. J. Haigh, *Int. Aerospace and Ground Conf. on Lightning and Static Electricity (Paris, 2007)*

4. “Assessment of lightning direct effects damages by modeling techniques”, P.N. Gineste, R. Clerc, C. Castanié, H. Andreu, E. Buzaud, *Int. Aerospace and Ground Conf. on Lightning and Static Electricity (Pittsfield, 2009)*

5. “Physical study of laser-produced plasma in confined geometry”, R. Fabbro, J. Fournier, P. Ballard, D. Devaux, J. Virmont, J. Appl. Phys. **68** (1990) 775

6. “Physical Properties of High-Pressure Plasmas of Hydrogen and Copper in the Temperature range 5000-60000”, P. Kovitya,

IEEE Trans. Plasma Science, PS-13, p. 587 (1985).

Acknowledgments

We thank “DGA Techniques Aéronautiques” (Toulouse) for performing the lightning tests on the ElectroMagnetic Means for Aerospace (EMMA) platform. The visars and high speed camera were provided and operated by the “detonics mechanics and thermics” CEA team (Gramat). We also thank Dr. F. Flourens and Dr. R. Murillo from Airbus for their continuous support of this work.